Biochimica et Biophysica Acta 1857 (2016) 1569–1579

Contents lists available at ScienceDirect

Biochimica et Biophysica Acta

journal homepage: www.elsevier.com/locate/bbabio

From low- to high-potential bioenergetic chains: Thermodynamic constraints of Q-cycle function

Lucie Bergdoll [a,1], Felix ten Brink [b], Wolfgang Nitschke [b], Daniel Picot [a], Frauke Baymann [b,*]

[a] Institut de Biologie Physico-Chimique, Unité Mixte de Recherche 7099, Centre National de la Recherche Scientifique, Université Paris Diderot, 13 Rue Pierre et Marie Curie, 75005 Paris, France
[b] Centre National de la Recherche Scientifique, Aix-Marseille Univ, Laboratoire de Bioénergétique et Ingénierie des Protéines, Institut de Biologie Structurale et Microbiologie, Unité Propre de Recherche 7281, FR3479, 31 Chemin Joseph-Aiguier, 13402 Marseille Cedex 20, France

ARTICLE INFO

Article history:
Received 21 March 2016
Received in revised form 14 June 2016
Accepted 16 June 2016
Available online 17 June 2016

Keywords:
Q-cycle
Rieske/cyt*b* complex
Cytochrome bc_1 complex
Quinone
Electron bifurcation
Great Oxidation Event

ABSTRACT

The electrochemical parameters of all cofactors in the supercomplex formed by the Rieske/cyt*b* complex and the SoxM/A-type O_2-reductase from the menaquinone-containing Firmicute *Geobacillus stearothermophilus* were determined by spectroelectrochemistry and EPR redox titrations. All redox midpoint potentials (E_m) were found to be lower than those of ubi- or plastoquinone-containing systems by a value comparable to the redox potential difference between the respective quinones. In particular, E_m values of +200 mV, −360 mV, −220 mV and −50 mV (at pH 7) were obtained for the Rieske cluster, heme b_L, heme b_H and heme c_i, respectively. Comparable values of −330 mV, −200 mV and +120 mV for hemes b_L, b_H and the Rieske cluster were determined for an anaerobic Firmicute, *Heliobacterium modesticaldum*. Thermodynamic constraints, optimization of proton motive force build-up and the necessity of ROS-avoidance imposed by the rise in atmospheric O_2 2.5 billion years ago are discussed as putative evolutionary driving forces resulting in the observed redox upshift. The close conservation of the entire redox landscape between low and high potential systems suggests that operation of the Q-cycle requires the precise electrochemical tuning of enzyme cofactors to the quinone substrate as stipulated in P. Mitchell's hypothesis.

1. Introduction

All life on this planet crucially depends on energy harvesting, that is, the ability to convert environmental sources of free energy into chemical disequilibria to drive metabolic reactions. Most unicellular organisms and certainly all complex ones use a unique mechanism for energy harvesting: chemiosmosis. A wealth of phylogenetic evidences indeed suggests that the roots of the chemiosmotic mechanism reach as far back as the last universal common ancestor (LUCA) of Archaea and Bacteria (reviewed in [1]) and possibly even as far as life's ultimate origin [2]. The fundamental principles of chemiosmosis in mitochondria, the powerhouses of eukaryotic cells, have been worked out several decades ago in the pioneering work of Peter Mitchell [3]. Despite the availability of 3D structures of all key enzymes involved in aerobic respiration and an overall agreement on their function molecular details of their catalytic turnovers and the mechanism of ion-gradient build-up are still matters of intense controversy [4–9].

Rieske/cyt*b* complexes[2] are among the enzymes of the bioenergetic reaction chain that are present in most organisms. They integrate the chain at the level of quinones, their substrate. Depending on the organism the quinone can either be menaquinone, a naphthoquinone derivative with a redox midpoint potential of about −70 mV or one of the high potential quinones (ubiquinone, plastoquinone or calderiellaquinone) at

* Corresponding author.
E-mail addresses: Lbergdoll@mednet.ucla.edu (L. Bergdoll), nitschke@imm.cnrs.fr (W. Nitschke), picot@ibpc.fr (D. Picot), baymann@imm.cnrs.fr (F. Baymann).
[1] Present address: Department of Physiology, David Geffen School of Medicine, University of California Los Angeles, 10833 Le Conte Avenue, Los Angeles, California 90095-1751, USA.

[2] As pointed out several times in the past, the nomenclature with respect to the different versions of the Q-cycle enzyme in various species is inconsistent. The terms bc_1 and b_6f complexes historically refer to subunits carrying cofactors visible in optical spectroscopy and therefore having been the first to be identified, whereas one of the key players in enzyme turnover, the Rieske centre, does not figure in these terms. The structurally unrelated c_1 and *f*-heme subunits are not directly involved in catalysis and are in other Q-cycle enzymes replaced by further structurally unrelated *c*- and *b*-type heme subunits or putatively even by cupredoxins in some Archaea whereas in Chlorobiacea this subunit is absent. We therefore prefer to use the term "Rieske/cyt*b*-complexes", emphasizing their functionally crucial cofactors, when referring to the enzyme family in general. When addressing a specific subfamily, the *c*-type subunit indeed may serve as a distinguishing parameter and we therefore either use the bc_1 and b_6f terms for proteobacterial/mitochondrial and cyanobacterial/chloroplast enzymes, respectively, or keep the principle of using the names of the *b*- and the *c*-type subunits while adapting to the specific cases under consideration. Furthermore, we use b_6 to indicate presence of a gene-split in the membrane subunit which frequently goes along with the presence of heme c_i as opposed to the bulk of cytochromes *b* in Rieske/cyt*b* complexes which are devoid of this additional heme cofactor. The Rieske/cyt*b* complex from *G. stearothermophilus* therefore is called b_6c, that of *H. modesticaldum* b_6cc while that in *C. glutamicum* would be referred to as *bcc* (with the "cc" in both cases indicating that the *c*-subunit is a diheme protein).

http://dx.doi.org/10.1016/j.bbabio.2016.06.006
0005-2728/

about +100 mV [10–12]. Distribution of quinones among species [1,13] and phylogenetic evidence [14–17] indicate that menaquinones were present first in evolution. High-potential quinones probably evolved later in response to the increase in the environmental redox state brought about by rising O_2 levels during the so-called Great Oxidation Event (GOE) about 2.5 billion years ago [18].

Peter Mitchell based his Q-cycle mechanism uniquely on the thermodynamic properties of the quinones and the redox centres of the responsible enzyme, the bc_1 complex, in the context of an energized membrane. Ever since numerous variants of the original proposal have been published and despite an overall agreement on enzyme function the mechanistic and electrochemical determinants of bifurcated quinol-oxidation remain highly contentious [4,5,7,19]. In addition many authors consider minimization of ROS-generating side-reactions [4,20–22] as an evolutionary driving force that shapes the redox potentials of the cofactors of the complex in aerobic environments.

The comparison of Rieske/cyt*b* complexes from organisms thriving on high- or on low-potential quinones in aerobic or anaerobic environments appears as a promising strategy to tease apart thermodynamic properties fundamental to Q-cycle function from characteristics which evolved in order to mitigate ROS formation.

On present day earth, PQ and UQ containing organisms dominate the macroscopic biosphere and their Rieske/cyt*b* complexes are well characterized. The overwhelming majority of prokaryotes, however, still thrive on bioenergetic reaction chains based on MK only. Despite their wide phylogenetic distribution, MK-organisms are only little studied. While redox data have been reported for specific cofactors in a plethora of menaquinone-based chains [23–28], none of these systems features a complete-enough dataset to allow detailed comparison with the ubi- and plastoquinone systems of mitochondrial/proteobacterial respiration and of oxygenic photosynthesis.

Bacilli, members of the Firmicutes, exclusively contain menaquinone and are known to harbour high concentrations of bioenergetic enzymes some of which even form supramolecular assemblies which persist during solubilization [29]. Such a case is present in *Geobacillus* (*G.*) *stearothermophilus* which we therefore chose for characterizing a biochemical isolate of an entire electron transfer chain from menaquinone to oxygen, including a Q-cycle enzyme, a membrane anchored mono-heme cytochrome *c* and a *caa*(o)$_3$-type O_2 reductase (Fig. 1A). Combining these results with the ensemble of data available on other low potential Q-cycle enzymes as well as on the better studied high-potential systems yields valuable information on variability and conservation of thermodynamic driving forces within the enzyme family and within the entire bioenergetic electron transfer chain.

2. Materials and methods

2.1. Sample preparation

Geobacillus stearothermophilus was grown in 2YT medium at 55 °C at a pO_2 above 70%. Membranes were solubilized by *n*-Dodecyl beta-D-maltoside in 20 mM TrisHCl pH 8 (w/w ratio protein:detergent 1.6:1) at room temperature for 45 min, loaded on a Q ceramic column (Pall) and eluted with a linear NaCl gradient. Fractions containing the supercomplex eluted at around 200 mM NaCl, and were loaded on a 10%–30% sucrose gradient and centrifugated at 4 °C, for 15 h at 37,864*g*. The band corresponding to the supercomplex was loaded on a HTQ 5 ml column (GE healthcare) and eluted with a NaCl gradient at

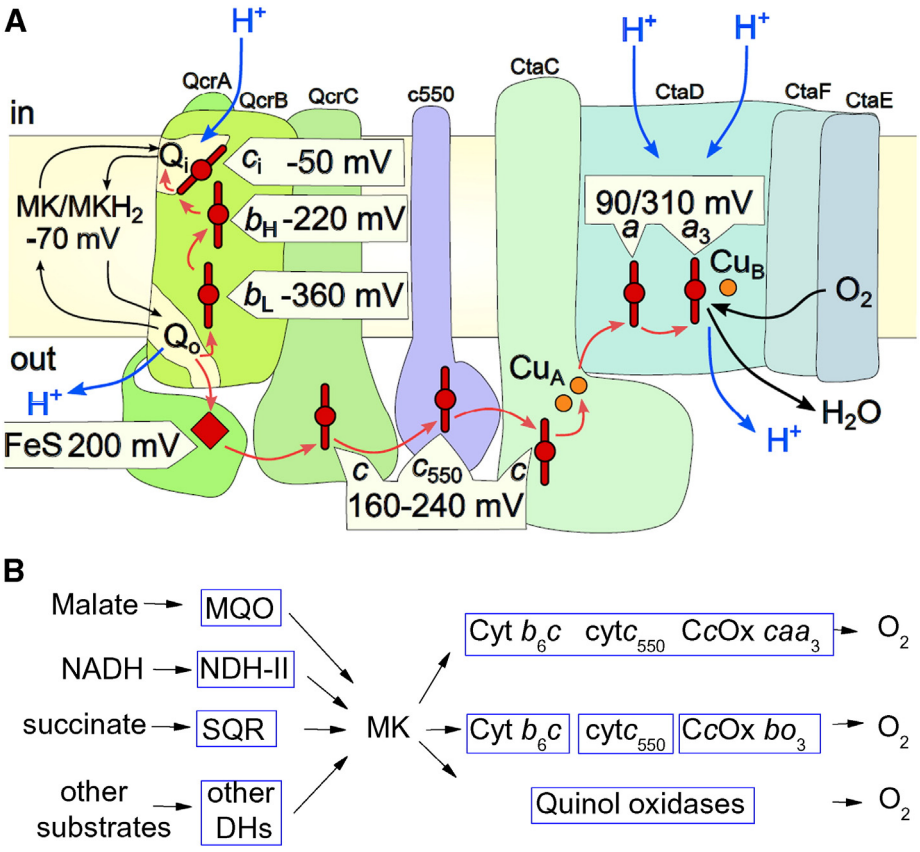

Fig. 1. A: Schematic representation of the supercomplex of *Geobacillus stearothermophilus*. Electron and proton movements during the MKH_2 to O_2 reaction are indicated by red and blue arrows, respectively. Redox midpoint potentials of the cofactors, as determined in this work, are marked. B: The different respiratory chains of *Geobacillus* as expressed in response to different environmental conditions.
(Adapted from [77]).

200 mM NaCl, dialyzed and reinjected on the same column. The eluted fractions were pooled and concentrated (100 kDa cut-off centricon (millipore)). Hemes *a* and *c* concentrations were determined from ascorbate-reduced minus oxidised difference spectra and the heme *b* concentration from dithionite-reduced minus ascorbate-reduced difference spectra. Extinction coefficients of 11.6 mM^{-1} cm^{-1} [30], 21 mM^{-1} cm^{-1} [30,31], and 20 mM^{-1} cm^{-1} [32] were used for the α-bands of hemes *a*, *b* and *c* respectively.

H. modesticaldum was grown anaerobically at 50 °C in DSMZ medium 655. Cultures were constantly illuminated by two 100 W light bulbs. Membranes were prepared from frozen cell material in 50 mM Mops buffer pH 7.

2.2. EPR spectroscopy

EPR spectra were recorded on a Bruker Elexsys E500 X-band spectrometer fitted with an Oxford Instrument He-cryostat ESR900 and temperature control system. Conditions are indicated in the figure legend.

Redox titrations were performed as described by [33] in the presence of the mediators 2.5-$(OH)_2$-*p*-benzoquinone, *N*,*N*,*N*′,*N*′-tetramethyl-*p*-phenylenediamine, mono-ferrocene, 2,6-dichlorophenol-indophenol, 1,2-naphthoquinone, cresyl blue, methylene blue, indigocarmine, anthraquinone-2,6-disulfonate, anthraquinone-2-sulfonate, safranine T, neutral red at 100 μM each. Reductive titrations were carried out using sodium dithionite, oxidative titrations using oxygen (injecting air) or ferricyanide. Protein concentration was approximately 10 μM.

2.3. Visible spectra and electrochemistry

Redox titrations of the purified supercomplex were performed using a thin-layer electrochemical cell adapted from [34] monitored by optical spectroscopy on a Cary 5E spectrophotometer. The Ag/AgCl electrode was calibrated against a saturated quinhydrone solution in 1 M MOPS buffer, pH 7 at RT (E_m + 280 mV) before each experiment. The mediators ferrocene, monoferrocene, ferricyanide, *p*-benzoquinone, 2,5-$(CH_3)_2$-*p*-benzoquinone, 1,2-naphthoquinone, 1,4-naphthoquinone, 2-(CH_3)-1,4-naphthoquinone, 2,5-di-OH-*p*-benzoquinone, anthraquinone-2,6-disulfonate, anthraquinone, benzyl viologen were added at a concentration of 20 μM each. Glucose/glucose oxidase was added to the sample to avoid possible redox disequilibria due to oxygen leakage into the cell. Titrations were performed in steps of 30 mV with an equilibration time of 2–10 min. The total duration of a titration was of up to 10 h. Redox titrations were always performed in oxidative and reductive direction to assure complete reversibility of redox behavior, indicative of equilibration of the sample with the applied potential and integrity of the sample over the entire duration of the titration. Protein concentration was 40 to 60 μM in the different experiments at pH 7 and around 15 μM for experiments at pH 9. Data were analyzed using in-house software for the determination of redox midpoint potentials and spectra of the individual compounds.

3. Results

Geobacillus stearothermophilus grown at high oxygen tensions as applied in our study predominantly expresses a *caa*$(o)_3$-type O_2-reductase associated with a Rieske/cyt*b*[2] complex in a supercomplex [29]. Similar to Sone and Fujiwara [35] we observed a heterogeneity in the heme content of the O_2-reductase's binuclear centre with minor contributions of heme O instead of heme A. Solubilization of membranes in *n*-Dodecyl β-D-maltoside and purification through a sucrose gradient followed by ion exchange chromatography allowed us to isolate this supercomplex comprising a cyt b_6c complex[2], a cyt caa_3-type O_2 reductase and a small monoheme cytochrome c_{550} (see Section 2 and Figs. 1A and 2). A comparable isolate had previously been reported for the related

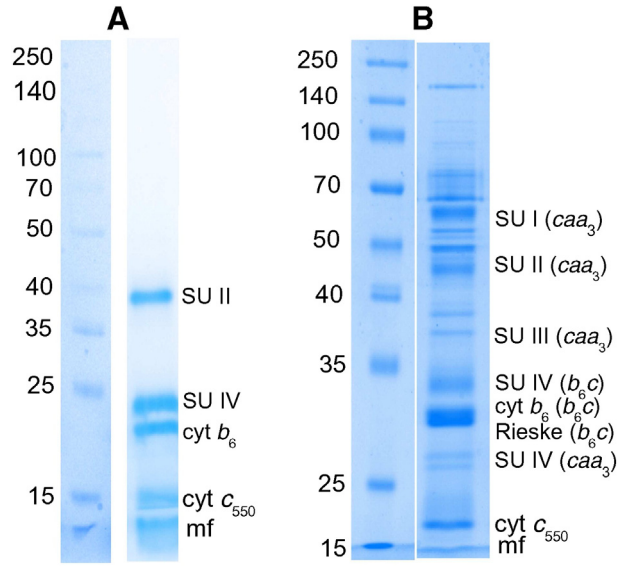

Fig. 2. SDS-PAGE of the supercomplex used for the electrochemical titrations. A: Heme-specific staining using TMBZ [78] confirms the presence of 4 *c*-type hemes in the sample. B: Coomassie blue staining reveals the presence of all known subunits of the supercomplex. Molecular markers are indicated on the left hand site of the gel and protein bands are attributed to the subunits of the Rieske/cyt*b*:caa_3 complex on the right hand side, mf: migration front.

Firmicute *Bacillus* sp. PS3 [29]. The samples we obtained via our purification procedure were sufficiently concentrated and stable to allow electrochemical redox titrations recorded in the visible spectral region as well as chemical redox titrations monitored by EPR spectroscopy. The combination of these two methods permitted the determination of all cofactors' redox midpoint potentials.

3.1. Redox midpoint potentials of the cofactors from the b_6c/$caa(o)_3$ complex of G. stearothermophilus

3.1.1. The Rieske centre

The Rieske iron sulphur cluster was monitored using low-temperature EPR spectroscopy (Fig. 3A). Both its g_x-trough and its derivative-shaped g_y-line titrated with a redox midpoint potential of +200 mV (Fig. 3B), i.e. close to the value reported for the *Bacillus* sp. PS3 enzyme [26]. This value is lower than the redox midpoint potentials observed in Rieske centres of UQ- and PQ-systems. The potential difference correlates with the number of hydrogen bonding residues (0, 1, or 2) in two conserved sequence positions [36]. In *G. stearothermophilus* a single tyrosine residues is present.

3.1.2. The b-type hemes

In contrast to iron sulphur clusters, low-spin heme cofactors are most conveniently observed by UV/vis spectroscopy. Fig. 4 shows redox-induced difference spectra of hemes *a*, *b* and *c* as deconvoluted by a global fit analysis from an electrochemical redox titration monitored by optical spectroscopy.

The dependence of signal size at different wavelengths on the applied ambient potential is visualized in Fig. 5A and D. Midpoint potentials of −360 mV and −220 mV were obtained for the two *b*-hemes of the b_6c complex (Fig. 5A) with distinct difference spectra in the α-band peaking at 564 nm for heme b_H and at 561 nm for heme b_L (Fig. 4). No significant pH dependence was detected between pH 7 and 9 (Fig. 5D, E).

The redox midpoint potentials for *b*-hemes are substantially lower than any so far reported values for this co-factor and lower also than those reported for the isolated b_6c complex from the closely related species *Bacillus* sp. PS3 [24]. The *Bacillus* sp. PS3 sample was purified using Triton X-100 as detergent. In plastidic b_6f complexes, Triton was

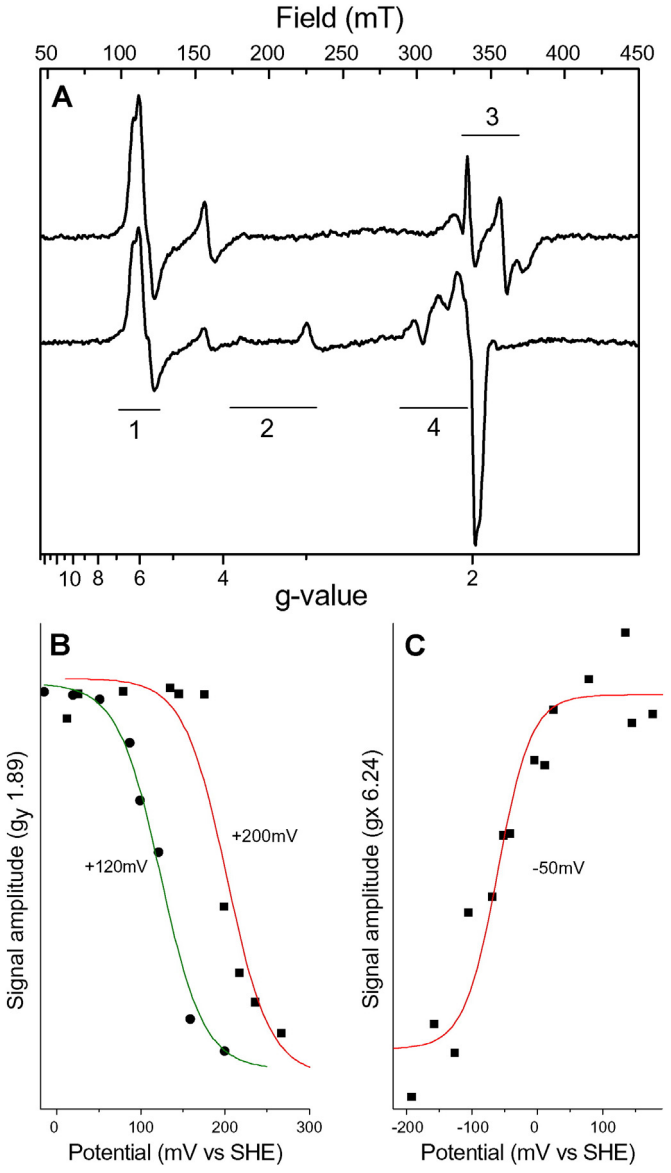

Fig. 3. A: EPR spectra of the isolated supercomplex: air-oxidised (bottom), ascorbate-reduced (top). The spectral region of the $g_{x,y}$ signals of the high-spin heme c_i (1), g_z of low spin hemes *a*, *c* and *b* (2), $g_{x,y,z}$ of the Rieske centre (top (3)) and $g_{x,y,z}$ of the copper (bottom (4)) are indicated. B: Redox titration of the Rieske g_y signal on *G. stearothermophilus*' purified supercomplex (squares) and *H. modesticaldum* membranes (circles) fitted to n = 1 Nernst curves (red *G. stearothermophilus*, green: *H. modesticaldum*). C: Redox titration of hems c_i's g_x signal on *G. stearothermophilus*' purified supercomplex, fitted to a n = 1 Nernst curve. EPR settings: temperature, 15 K; microwave power, 6.4 mW; microwave frequency: 9.48 GHz; modulation amplitude 0.00303 T.

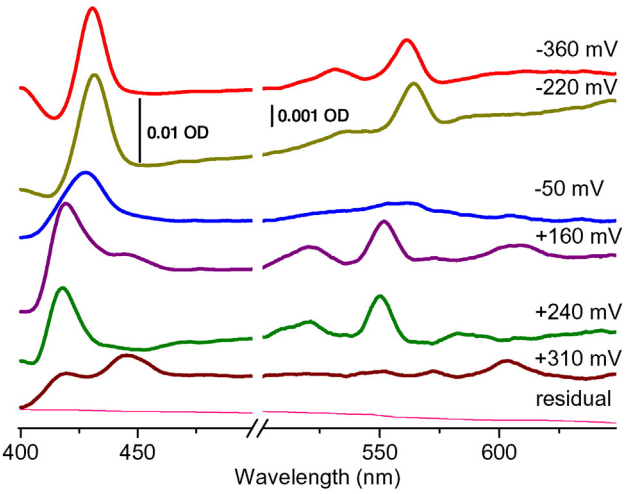

Fig. 4. Deconvolution of optical spectra recorded during a redox titration. Spectral components attributed to (from top to bottom): heme b_L (−360 mV), heme b_H (−220 mV), heme c_i (−50 mV), heme *c* and a/a_3 (+160 mV), heme *c* (+240 V), heme a/a_3 (+310 mV).

reported to strongly decrease enzymatic activity and to affect the E_m values of the *b*-hemes [37]. We consider that this fact and/or the experimental difficulties in exploring ambient potentials far below −200 mV in conventional chemical titrations may rationalize the E_m values published for *Bacillus* sp. PS3.

To assess whether the extraordinarily low potentials determined in the present study may be due to alterations/degradations brought about by our purification procedure we performed redox titrations directly on membranes from *G. stearothermophilus*. The thin layer electrochemical cell allowed us to monitor spectra on membranes over the entire visible spectral range with a low contribution of light scattering due to the short optical path length of 60 μm. In membranes complex II is present and features two *b*-heme in *G. stearothermophilus*. We purified complex II and titrated the redox midpoint potentials of the *b*-hemes from the purified enzyme to −170 mV and −5 mV (Fig. 6A, inset). In membranes, in the potential range explored we observe the low potential *b*-heme of complex II at −160 mV and further absorbance changes at lower redox potential that can be described by absorbance changes of two *b*-hemes with midpoint potentials at −280 mV and −375 mV (Fig. 6A). Taking into account the precision of the method (±20 mV), heme b_L shows the same redox midpoint potential in membranes and in the isolated supercomplex. Heme b_H features a somewhat lower redox midpoint potential in membranes.

3.1.3. Heme c_i

Heme-staining on SDS-PAGE revealed the presence of a heme covalently bound to the cytochrome b_6 subunit of the b_6c complex. This was indeed to be expected from the presence of a cysteine residue in the sequence position where the cysteine residue that covalently binds heme c_i is found in b_6f complexes. The presence of a covalently linked heme is in line with similar observations on *Bacillus subtilis* [38], *Bacillus* sp. PS3 [24] and Heliobacteria [39]. In chloroplasts [40,41], Cyanobacteria [12,42] and Heliobacteria [39], heme c_i has been shown to be high spin. In optical spectroscopy high spin hemes typically are characterized by broad and extremely weak α/β - but reasonably strong Soret-bands. In EPR, by contrast, high spin hemes distinguish themselves by very prominent signals (corresponding to their g_x and g_y lines) in the g = 6 field region of the spectrum due to the high transition probabilities of the S = 5/2 spin state.

In *G. stearothermophilus*, heme c_i gave rise to a broad Soret-type absorption band around 430 nm (Fig. 4) characteristic for a high-spin heme but slightly shifted with respect to the band observed for its homolog in the b_6f complex [40] which peaks at 425 nm. The absorption band titrated with −50 mV when measured at pH 7 (Fig. 5E). At pH 9, however, the redox midpoint potential had decreased to about −130 mV (Fig. 5D). Such a pronounced pH-dependence corresponds well to the steep pH-dependences observed for heme c_i in the b_6f complex [40].

The EPR spectrum of heme c_i (Fig. 3A) from *G. stearothermophilus* featured a split g_x signal with $g_{x1} = 6.05$, $g_{x2} = 6.26$ and a single g_y signal at 5.6. This structure is reminiscent of heme c_i's spectral shape in the b_6f complex when the inhibitor NQNO is present [41]. In the b_6f complex NQNO is considered to act as axial ligand to heme c_i. To do so, the inhibitor likely has to push away the phenylalanine residue which caps the axial coordination site of heme c_i exposed to the quinone binding pocket [43]. Sequence alignments suggest that this phenylalanine residue is replaced in Firmicutes by a glutamic acid [39] which could well act as a

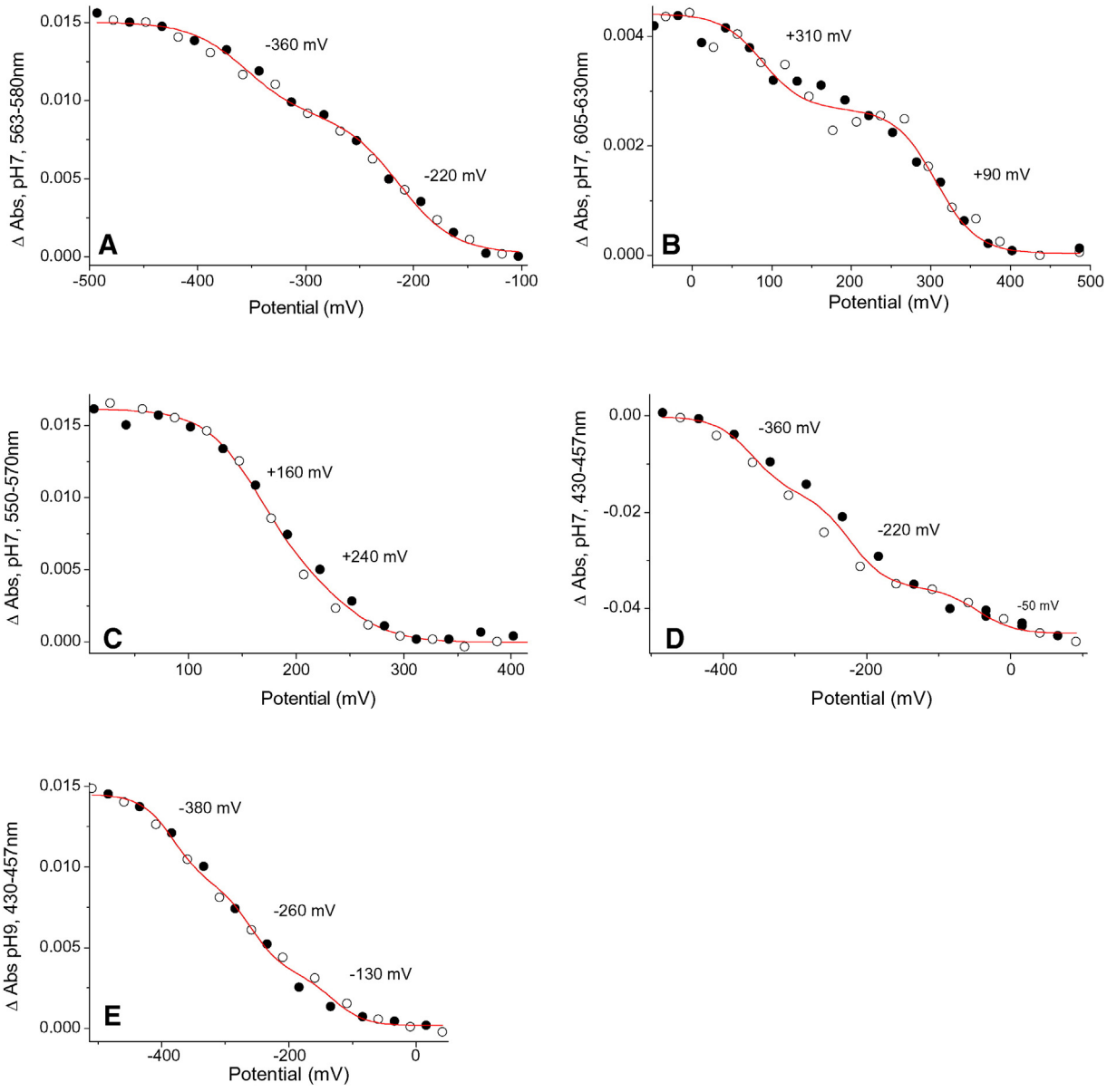

Fig. 5. Redox titrations of the purified b_6c:c_{551}:caa_3 from *G. stearothermophilus* at pH 7. A: α-Band of hemes *b* (563 nm–580 nm, E_m − 390 mV/−220 mV); B: α-band of hemes a/a_3 (605 nm–630 nm, E_m + 90 mV/+310 mV); C: α-band of hemes *c* (550 nm–570 nm, E_m + 160 mV/+240 mV); D: Soret band of hemes *b* and c_i (430 nm–457 nm, Em −360mV/–220mV/–50mV); E: Soret band of hemes *b* and c_i (430 nm–457 nm, Em –380mV/–260mv/–130mV) at pH 9. Open symbols stand for amplitudes measured during oxidative titration, full symbols for reductive titration, the red lines represents sums of n = 1 Nernst curves fitted to the data points.

ligand to heme c_i rationalizing the close resemblance between heme c_i's EPR spectrum of the *Geobacillus* complex to that of the NQNO-ligated form of the b_6f complex. The EPR signal titrated with −50 mV at pH 7 (Fig. 3C), similar to the optically determined redox potential at this pH value.

3.1.4. c-Type hemes

Judging from SDS-PAGE (Fig. 2) our supercomplex contains three different *c*-type hemes respectively belonging to the Rieske/cyt*b* complex, the caa_3/cao_3-type O_2-reductase and the monoheme cyt c_{550}. In our electrochemical titrations, *c*-type hemes were found to change redox state in a narrow range between +120 and +280 mV (Fig. 5C). All three hemes therefore feature E_m values between +160 and +240 mV and this strong overlap in redox midpoint potentials precludes an unambiguous attribution of individual values to each heme. However, the potentials where we see *c*-type hemes titrate in our supercomplex correspond well to those determined in more fractionated samples of *Bacillus* sp. PS3 for the monoheme cytochrome and the cytochrome subunit of the Rieske/cyt*b* complex at 225 mV and 200 mV, respectively [24,44]. Redox-difference spectra calculated from our titration data demonstrate that the α-peaks of all three hemes lie in the region between 550 and 551.5 nm.

3.1.5. Copper A

While copper A (Cu_A) signals are visible in the EPR spectrum of the oxidised sample (Fig. 3A), its redox potential unfortunately could not be evaluated due to strong overlap from the g_z-peak of the reduced Rieske centre, the g_y signals of oxidised *c*- and *b*-type hemes and spectral contributions from the redox mediators. We observed, however, that the Cu_A EPR-signals remain roughly unchanged down to +200 mV and only disappeared at lower potentials indicating a redox midpoint potential in this range.

3.1.6. Heme a and the binuclear centre

The redox transitions of heme *a* monitored on the 605 nm band were reversible and showed two titration waves with similar

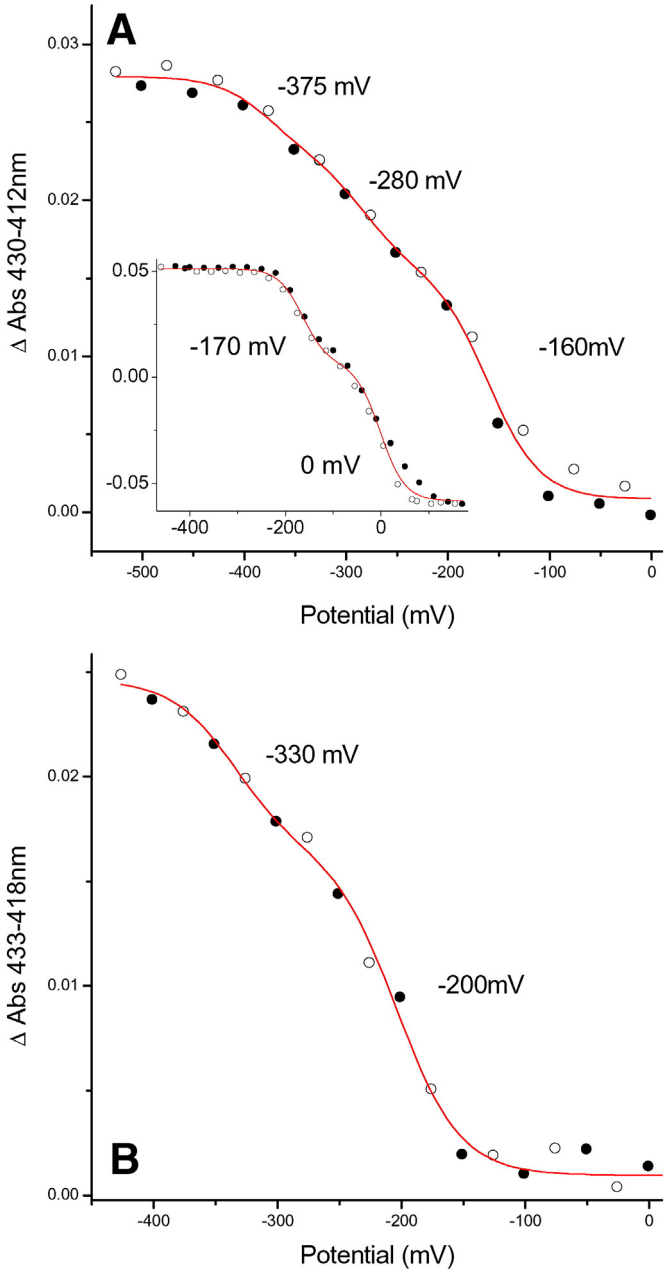

Fig. 6. Redox titrations on membranes from *G. stearothermophilus* and *H. modesticaldum*. A: Soret band of *b*-hemes from *G. stearothermophilus* (430–412 nm); the red line represents a fit to three n = 1 Nernst curves (Em −375 mV/−280 mV/−160 mV), the inset shows a redox titration of the *b*-hemes of the purified complex II of *G. stearothermophilus* (430-412 nm, Em −170 mV/0 mV). B: Soret band of *b*-hemes from *H. modesticaldum* (433–418 nm) fitted to a sum of two n = 1 Nernst curves (Em –330mV/–200mV). Open symbols stand for amplitudes measured during oxidative titration, full symbols for reductive titration.

amplitudes at +90 mV and +310 mV (Fig. 5B). Deconvoluted spectra for the individual redox components featured α-bands at 606 nm and 604 nm, respectively (Fig. 4). Two titration waves for heme *a* have been observed on other O_2-reductases and are considered to reflect electrostatic interactions of heme *a* with heme a_3/o_3 and Cu_B [45].

3.2. Redox midpoint potentials of Rieske/cytb complexes from other MK-organisms

The MK-system which comes closest to the *G. stearothermophilus* supercomplex with respect to completeness of available data is the anaerobic and anoxygenic photosynthetic chain of Heliobacteria [27,39,46]. The midpoint potential of heme c_i in these species is, however, more uncertain since (a) it has been measured on solubilized enzymes with altered redox properties of the *b*-hemes and (b) only half the amplitude of the signal attributed to heme c_i titrated according to a Nernst-curve [39]. In addition, our observation of extremely low E_m values for the *b*-hemes in *G. stearothermophilus* instilled doubts on the completeness of the redox titration published (among others by one of the authors of the present article) on membrane fragments from Heliobacteria [27]. In this redox titration, no data points were taken below −290 mV and the α-band spectral region on which the titration was evaluated in [15,27] is prone to confounding absorbance changes from the photosynthetic pigments. We therefore reexamined the electrochemical parameters of heliobacterial membranes using the spectroelectrochemical method also used for *G. stearothermophilus*, which allowed evaluation in the blue spectral region. We indeed found a much lower potential wave yielding substantially modified E_m values for b_L and b_H (−320 mV and −200 mV, respectively) in *Heliobacterium* (*H.*) *modesticaldum* (Fig. 6B). We titrated the Rieske cluster of this organism at +120 mV (Fig. 3B) in agreement with the value published on *Heliobacterium chlorum* [25].

In addition to *G. stearothermophilus* and *H. modesticaldum*, which are both members of the Firmicutes, comparatively low potentials, −160 mV for heme b_H and −290 mV for heme b_L, for the *b*-hemes in the Rieske/cyt*b* complex were more recently reported for *Corynebacterium* (*C.*) *glutamicum* (Table 1), an organism belonging to the phylogenetically distant Actinobacteria [47]. Finally, the redox midpoint potential of the Rieske cluster of the bc_1 complex from the gammaproteobacterium *Halorhodospira halophila* that operates in a menaquinone-based anaerobic photosynthetic reaction chain has been determined at +110 mV [16] (Table 1).

4. Discussion

Our spectroscopic and electrochemical experiments on the Rieske/cyt*b*:O_2-reductase supercomplex from *G. stearothermophilus* allowed the determination of redox potentials for all crucial cofactors involved in bioenergetic electron transfer from the menaquinone pool to the terminal electron acceptor, O_2. Comparisons to UQ- and PQ-based systems suggest that to first approximation the redox potentials of all cofactors are lower by about the same amount as the difference between the quinones' potentials. According to P. Mitchell's thermodynamic formulation of the Q-cycle, this might have been expected. Indeed, the Rieske cluster of numerous MK-organisms was reported to feature a correspondingly lower redox-midpoint potential, when compared to PQ- and UQ-systems, a fact interpreted on the basis of the Mitchellian cycle. However, the same did not seem to be true for the E_m values of the *b*-hemes [24,27] instilling doubts on the stringency of locked redox spacing as proposed by P. Mitchell for the mitochondrial system. Our data now show that a stringent conservation of redox midpoint potential spacing from the quinones to both heme *b* and the Rieske cluster is found within the phylogenetic variety of studied Q-cycle enzymes and therefore appears inherent to the enzymatic mechanism.

A more detailed analysis reveals that two parameters are particularly well conserved. The redox potentials of heme b_L and the Rieske cluster are always centred around the quinone potential and the redox potential difference between the *b*-hemes is constant in most enzymes. The redox potential difference between heme b_L and the Rieske cluster, by contrast, is variable (Fig. 6). In the following we will discuss the constant and variable parameters with respect to the thermodynamics of the Q-cycle, accommodation of heme c_i, adaptations to prevent electron transfer to oxygen and finally the integration of the enzyme in the redox profile of a bioenergetic reaction chain.

Table 1
Overview of redox midpoint potentials and K_S value discussed in this article.

Organism	E_m Rieske	E_m b_H	E_m b_L	E_m c_i	K_S Q_o	Quinone
G. stearothermophilus	+200 mV	−220 mV	−360 mV	−50 mV	n.d.	MK −70 mV
H. modesticaldum	+120 mV	−200 mV	−330 mV	ca −50 mV*	n.d.	MK −70 mV
H. halophila	+110 mV	n.d.	n.d.	/	n.d.	MK −70 mV
C. glutamicum	n.d.	−163 mV	−291 mV	/	n.d.	MK −70 mV
R. sphaereoides	+285 mV	+50 mV	−88 mV	/	10^{-14}–10^{-15}	UQ +90 mV
S. cerevisiae	+285 mV	+82 mV	−60 mV	/	n.d.	UQ +90 mV
R. capsulatus	+274 mV	+40 mV	−89 mV	/	n.d.	UQ +90 mV
C. reinhardtii	+330 mV	−35 mV	−130 mV	+100 mV	n.d.	PQ +115 mV
A. aeolicus	+210 mV	−60 mV	−190 mV	/	n.d.	DMK 0 mV

Experimentally determined redox midpoint potentials of quinones and the cofactors of selected Rieske/cyt*b* complexes discussed in this article UQ: [70], PQ: [11], MK: [71], DMK: [48]. bc_1 complex from *R. sphaeroides*: [72,73]; bc_1 complex from *S. cerevisiae*: [74,75]; bc_1 complex from *R. capsulatus*: [76]; b_6f complex from *C. reinhardtii*: [40] and our unpublished results for the Rieske cluster; bc_1 complex from *A. aeolicus*: [49]; b_6c complex from *G. stearothermophilus*: this work; b_6cc complex from *H. modesticaldum*: [39] and this work; * preliminary results: only half of the amplitude of the signal titrated at this value; *bc* complex from *H. halophila*: [16]; *bcc* complex from *C. glutamicum*: [47]; n.d.: not determined; / complexes do not feature heme c_i.

4.1. E_m values of b_L and the Rieske cluster are symmetrically spaced around the quinone potential

Fig. 7 visualizes the redox midpoint potentials of the cofactors of Rieske/cyt*b* complexes from a variety of species and of their substrate quinones. The redox midpoint potentials of heme b_L and the Rieske cluster are always arranged symmetrically below and above the midpoint potential of their physiological reductant, the quinone. Such a symmetrical spacing was previously found in the bc_1 complexes of mitochondria and Alphaproteobacteria and in b_6f complexes from chloroplasts and Cyanobacteria, i.e. for the enzymes reacting with high potential UQ and PQ. Our results now establish the same redox pattern for enzymes reacting with low-potential MK. An interesting intermediate case is provided by the organism *Aquifex aeolicus*, a member of the deeply branching Aquificales. This species was shown to contain demethylmenaquinone (DMK) as pool quinone [48]. DMK features an E_m value in the range of 0 mV [48] which is in between those of the traditional low and high potential quinones. Also in this case heme b_L and the Rieske cluster exhibit potentials symmetrically arranged around that of their quinone ([49], Table 1 and Fig. 7).

Q_o-site turnover is characterized by two basic observations: (a) the individual electron transfer reactions at Q_o towards the iron sulphur centre on one side and heme b_L on the other side observed both in bc_1 and b_6f complexes are strongly coupled; (b) the reduction of the Rieske centre by the quinol/semiquinone couple has been found to be the rate-limiting step of enzyme turnover in all enzymes studied to this respect [4,27]. Both these observations are frequently rationalized by the peculiar redox chemistry of quinones and in particular by their tendency to undergo cooperative 2-electron redox reactions in aqueous solutions [4,7,50]. Detailed mechanistic scenarios for this Q_o-site turnover have

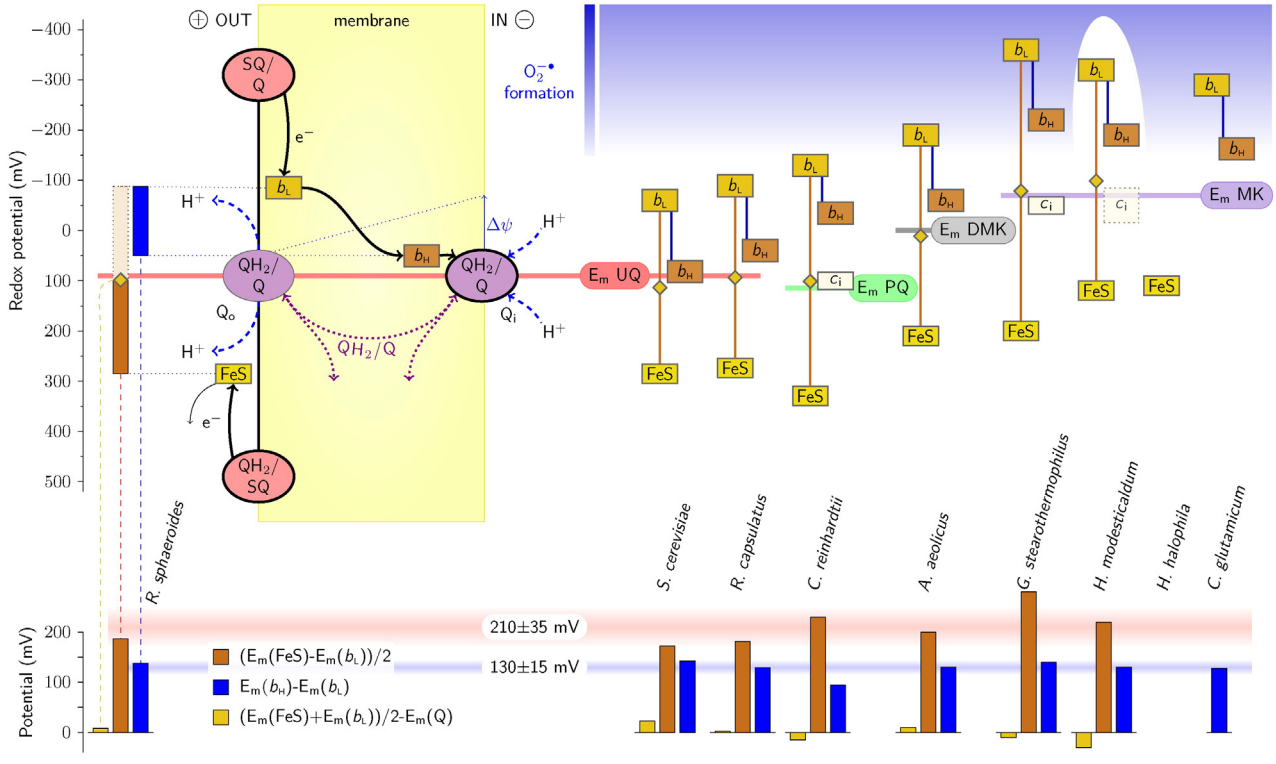

Fig. 7. Schematic representation of the redox landscape of the Rieske/cyt*b* complexes from different organisms. Top left: schematic representation of the Q-cycle for the bc_1 complex of *Rhodobacter sphaeroides* with all redox midpoint potentials of the cofactors involved. Top right: overview of known redox midpoint potentials of different species: horizontal lines indicate the redox midpoint potentials of the quinones, rectangles depict the redox midpoint potentials of the cofactors (yellow: Rieske cluster, white: heme c_i, light orange: heme b_L, dark orange: heme b_H) that have been experimentally determined, the blue shaded area at the top indicates redox potentials that lead to reactions with O_2. Driving force of the Q_o site reaction is illustrated by yellow diamonds. Bottom: crucial parameters for Q-cycle function are depicted as columns: orange: driving force for enzyme turnover, blue: driving force of transmembrane electron transfer in the absence of $\Delta\Psi$, yellow: driving force of the Q_o-site reaction.

been elaborated based on data gathered on Alphaproteobacteria [4,20]. These scenarios feature strongly inverted potentials of the individual redox transitions, i.e. an E_m value for the first electron leaving the quinone and reducing the Rieske centre which is substantially more positive than that of the second electron reducing heme b_L. The intermediate SQ state therefore is destabilized according to log $K_S = \Delta E * F / RT$ (with ΔE corresponding to the redox span between the first and the second quinone oxidation steps and K_S to the stability constant of the semiquinone). Equilibrium concentrations of the semiquinone therefore are too low to be picked up in redox titrations of wild-type Rieske/cyt*b* complexes and the two 1-electron redox potentials cannot be determined straightforwardly through equilibrium redox titrations. A wide range of K_S values (and respective 1-electron E_m values) has been proposed to be in line with Q-cycle functioning [20]. Redox titrations of mutant enzymes [12] and kinetic experiments on inhibited complexes [4], however, allowed to estimate K_S values in the region of 10^{-14} to 10^{-15} for bc_1 complexes of Alphaproteobacteria. The corresponding split in E_m values between the single electron transitions amounts to 800–900 mV (indicated in Fig. 7 for *Rhodobacter sphaeroides*). Under such conditions, reduction of the Rieske cluster by the quinol is strongly endergonic and the electron will therefore mostly reside on the quinol. Only if the second electron, i.e. from the semiquinone/quinone couple, can perform the exergonic reduction of heme b_L will the full oxidation of quinol be thermodynamically feasible. Our observation of a symmetrical arrangement of heme b_L and the Rieske centre with respect to the quinone substrate also in the menaquinone-based Rieske/cyt*b* complexes strongly supports the universal validity of the above described thermodynamic coupling of the two individual electron transfer reactions at the Q_o-site.

The roughly symmetrical arrangement implies a nominal driving force for the bifurcated 2-electron oxidation of quinol at the Q_o-site (leading to the 1-electron reduction of both the iron-sulphur centre and heme b_L) which is close to nil in all systems studied (yellow column in Fig. 7, bottom) and indicates that these enzymes may be redox-poised for facile reversibility. It is noteworthy that the effective driving force may become slightly positive if the redox potential up-shift of the Rieske cluster in its position close to the Q_o site, observed on mutants of the hinge region in *bc* complexes [51], turns out to be a general property of the enzyme. The operating E_m of the quinone in the Q_o-site may also deviate from that of the bulk due to dissimilar binding affinities of the oxidised and reduced forms to the site. Slightly modified potentials as reported for several systems [26,52], however, mainly affect single turnover equilibria and rates whereas the potential of the bulk of quinones and the overall potential of the Rieske cluster will determine the equilibria of steady state throughput.

4.2. Heme c_i

The X-ray structures of cyt b_6f complexes from Cyanobacteria and chloroplasts [43,53] toppled the notion of a fully conserved scheme of catalytically crucial cofactors of Rieske/cyt*b* complexes. The b_6f complexes indeed turned out to contain an additional cofactor, heme c_i (also called c_n), located close to heme b_H in the Q_i-site and thus towards the n-side of the bioenergetic membrane (Fig. 1A). Unfortunately, the reaction details of quinone reduction at the Q_i-site, necessarily involving both heme b_H and heme c_i, remain enigmatic to the present day.

G. stearothermophilus represents only the second system so far for which a value for heme c_i's redox midpoint potential has been obtained to sufficient accuracy. Importantly, it is the first such system which is based on menaquinone whereas the previously reported E_m for heme c_i was measured in a green alga, i.e. an organism which uses the high potential plastoquinone [40,41]. For both the PQ- and the MK-systems heme c_i titrates close to the midpoint potential of the respective pool quinone. Disconcertingly, in both systems heme c_i displays a strong pH-dependence of E_m approaching 60 mV/pH. Such a pH-dependence is quite unusual for a heme cofactor and raises the possibility that the observed dependence of the optical and EPR spectra on ambient potential may in fact report the redox transition of a quinone molecule in the Q_i site. From the 3D structure and the study of inhibitor effects on heme c_i [40,41] it was concluded that this cofactor likely represents the immediate electron donor to the quinone which may even transiently form an axial ligand to the heme. The possibility that the Q_i site quinone and heme c_i form a redox-interacting couple should be considered when building future models on Q_i site turnover.

One of the most obvious dissimilarities in the comparison of complexes with and without heme c_i, irrespective of whether they react with MK or PQ/UQ, lies in the driving force for electron transfer from heme b_H to the quinone at Q_i (Fig. 7). As for our discussion of the Q_o site's thermodynamics, we will only consider the bulk potential of the quinone pool while acknowledging that the E_m values for the two redox transitions of the quinone molecule bound at Q_i may somewhat deviate [52] from the 2-electron value of the quinone pool. In a clear trend, the driving force for quinone reduction from heme b_H is significantly higher in the enzymes harbouring the additional cofactor heme c_i in their Q_i site. This is linked to a lower redox potential of heme b_H and b_L relative to the quinone potential and a correspondingly higher redox potential of the Rieske cluster and therefore probably a decreased stability constant of the Q_o site semiquinone as discussed in Section 4.4. The lack of a clear understanding of heme c_i's role in the Q_i site reaction unfortunately precludes a detailed interpretation of this conspicuous correlation at the time being.

4.3. The potential difference between hemes b_H and b_L is conserved

The spacing of redox potentials between hemes b_L and b_H appears astonishingly constant at around 130 mV in Rieske/cyt*b* complexes no matter whether they react with MK or high potential quinones. The so far only notable excursion to a lower value (100 mV) is observed in the b_6f complex (Fig. 7). This redox potential difference is traditionally interpreted as necessary [54] to allow for the electron to cross the membrane via the two *b*-hemes and against the electrostatic part ($\Delta\psi$) of the proton-motif-force (pmf). The 3D structures of the bc_1 and b_6f complexes indeed showed that electron transfer between hemes b_L and b_H corresponds to a movement of negative charges across the membrane dielectric in a trajectory almost perfectly perpendicular to the membrane plane and hence antiparallel to $\Delta\psi$. In an increasingly energized bioenergetic membrane, $\Delta\psi$ will therefore progressively reduce the driving force for electron transfer from heme b_L to heme b_H. The reduction of the Rieske centre by the quinol/semiquinone couple is the rate-limiting step of enzyme turnover in all enzymes studied to this respect [4,27]. The second electron issued from this quinol oxidation therefore has time to equilibrate within the b_L-b_H-Q_i-segment (for the case of complexes devoid of heme c_i) according to the cofactors' redox potentials while the redox equilibration between the quinol and the Rieske centre develops. E_m values in the low potential chain indicate that this equilibrium is strongly biased towards the Q_i-site in the absence of pmf and thus drives the entire Q-cycle in the forward direction. The electrostatic backpressure from $\Delta\psi$ in a fully energized membrane, however, will induce equilibria with substantial shares on heme b_L. Since all redox equilibria in the low potential chain occur faster than equilibration between the quinol and the Rieske centre, $\Delta\psi$-induced build-up of reduced heme b_L will favor the reversal of electron bifurcation at Q_o as long as an electron is present on the Rieske cluster. Alternatively, if a quinol occupies the Q_o site adjacent to an oxidised Rieske cluster reduction of the cluster by the first electron from the quinol could lead to reoxidation of heme b_L by the strongly oxidising semiquinone, a scenario very much reminiscent of the "broken Q-cycle" reaction reported for mutants of the b_6f complex [55]. Finally, if quinone is present in the Q_o site close to an oxidised Rieske cluster or a Rieske cluster in its distal position, electron transfer from b_L via the quinone to O_2 may occur [5,56,57] All these Q_o site reactions would interrupt transmembrane electron transfer when the part of

$\Delta\psi$ corresponding to the dielectric distance between these hemes starts to exceed the difference of b_L's and b_H's E_m values. The low potential chain of Rieske/cyt*b* complexes may thus be likened to a Zener-diode limiting the relative share of $\Delta\psi$ to total pmf. It should be kept in mind that in the last two of the above described scenarios forward electron transfer through the so-called high potential chain formed by the Rieske centre and heme c_1 is still possible while the membrane potential counteracts electron transfer across the membrane.

A noticeable deviation from the constant value of redox span between the two *b*-hemes is observed in the b_6f complexes. Intriguingly, however, the oxygenic electron transfer chain of chloroplasts appears to feature a lower contribution of the electrostatic component $\Delta\psi$ to total pmf and, consequently, a higher one of the osmotic term [58]. An even more extreme example of a system deviating from the common value shown in Fig. 7 is provided by the bioenergetic chain of the acidophile *Acidothiobacillus ferrooxidans*. In this species, pmf takes on values not very different from those measured in mitochondria or purple bacteria but the distribution onto ΔpH and $\Delta\psi$ differs substantially with a strongly dominant ΔpH but a small and even polarity-inverted $\Delta\psi$ [59,60]. In line with the reasoning outlined above, b_L and b_H have been found to be almost isopotential under physiological pH conditions and in the absence of $\Delta\psi$ in this organism [61].

In conclusion we would argue for a functional role of the b_L/b_H redox span, based on the observed conservation of the b_L/b_H redox difference in all presently characterized Rieske/cyt*b* complexes and on the correlation of the few deviant cases to deviant $\Delta\psi$ values. This notion was recently challenged by Pintscher and coworkers [62] who reported that bc_1 mutants featuring roughly isopotential *b*-hemes were still able to support photosynthetic growth and electron transfer from quinol to cytochrome *c*. These mutants are a system of choice to assess the functional role of the observed constant *b*-heme redox span by investigating their ROS production, the contribution of the mutated bc_1 complex to the build-up of the pmf and the share of $\Delta\psi$ on overall pmf as well as occurrence of linear electron flow through the high potential chain partially uncoupled from transmembrane transfer through the *b*-hemes.

4.4. Evolutionary adaptations driven by the threat of 1-electron reduction of O_2

The severe biological impact of ROS production partially due to Q_o-site reactions as established for bc_1 [63–65] and also observed for b_6f complexes [66] raises the questions of evolutionary adaptations to the presence of O_2. Bearing in mind the above described stringent thermodynamic constraints of the Q-cycle we will now discuss electrochemical details of enzyme function that may have evolved in response to O_2. When comparing the adaptations of organisms with high potential quinones to those living on MK, *G. stearothermophilus* and *H. modesticaldum* represent two organisms of choice since Heliobacteria are obligate anaerobes whereas *Geobacillus* appears to use its Rieske/cyt*b* complex exclusively in bioenergetics based on O_2-respiration (Fig. 1B).

The progressive blue shading at the top of the redox scheme in Fig. 7 denotes the region of redox potentials where the 1-electron reduction of O_2 to superoxide ($O2^{\bullet -}$) becomes thermodynamically favorable. As an approximate redox-limit for this reaction we have chosen the midpoint potential of the couple of dissolved O_2 and $O_2^{\bullet -}$ at atmospheric pressures (~−150 mV) as proposed by Wood [10,67]. In line with experimental evidence [63], cofactors of high potential quinone systems feature midpoint potentials above the perilous range to the exception of the semiquinone/quinone couple at Q_o (Fig. 7). The same doesn't hold for MK-based systems where both reduced hemes b_L and b_H feature sufficiently low E_m values to readily react with O_2. This suggests a rationale for the astonishingly similar E_m up-shifts of the various high potential quinones some of which are even chemically unrelated among each other: due to the interdependent redox midpoint potentials of the co-factors of the enzyme the up-shift of the quinone potential to roughly +100 mV will take the *b*-hemes out of the perilous redox region below −150 mV.

However, how do organisms which didn't evolve to use high potential quinones cope with the presence of O_2 in the biosphere? The redox midpoint potentials of their *b*-hemes and of the Q_o site semiquinone are in a range where one-electron reduction of O_2 should be possible (Fig. 7), although no experimental data on ROS production by Rieske/cyt*b* complexes from MK-species are as yet available. Comparing the Q-cycle enzyme of a strictly anaerobic organism, *H. modesticaldum*, to that of *G. stearothermophilus* which functions in O_2 respiration shows that the redox potential difference between the Rieske centre and heme b_L in *Geobacillus* largely exceeds the respective value observed in Heliobacteria and, as discussed above, the K_S value of the Q_o-site semiquinone therefore likely is substantially smaller in *G. stearothermophilus*. The consequently shorter lifetime of the semiquinone will reduce the probability of $O_2^{\bullet -}$ generating electrons leaking out of the Q_o-site and likely vastly compensate the inconvenience of an even lower E_m value of the semiquinone/quinone couple and of heme b_L. Corresponding dissimilarities in splitting of the Rieske centre's and heme b_L's E_m values between the b_6f complexes of oxygenic photosynthesis and bc_1 complexes from the oxygen consuming respiratory chain have been noted already several decades ago [68] and were proposed to protect the Q_o-site quinone against the higher O_2-concentrations generated by PSII by diminishing its K_S. Our results therefore indicate that lowering the Q_o site semiquinone's K_S to limit superoxide production is a common strategy adopted by *G. stearothermophilus* and by Cyanobacteria.

The same strategy is not observed in Rieske/cyt*b* complexes devoid of heme c_i as for example the MK-using *bcc* complex from the strictly aerobic *Corynebacterium glutamicum* (Fig. 7 and Table 1). Further research is necessary to find out how these organisms cope with the danger of ROS production by their Rieske/cyt*b* complexes.

4.5. Integration of the Rieske/cytb complex in a bioenergetic reaction chain

Rieske/cyt*b* complexes do not interact with external substrates and bioenergetic reaction chains containing a Rieske/cyt*b* complex therefore always fall into at least three functionally distinct entities, i.e. an enzyme injecting electrons into the quinone pool, the Rieske/cyt*b* complex channeling electrons from the membrane-integral quinones to periplasmic electron carrier proteins and finally a terminal reductase as electron exit module.

The aerobic respiratory chain from NADH to O_2, present in UQ-using mitochondria and in the MK-organism *G. stearothermophilus* is one example of such a chain. We discussed the adaptation of the Rieske/cyt*b* complex to the redox midpoint potential of the quinone (Section 4.1) and the possible adjustments made to cope with the presence of oxygen (Section 4.4) and found that an increase in the quinone midpoint potential results in a commensurable increase of the redox midpoint potentials of all cofactors of the complex and thereby takes the *b*-hemes out of the zone where single electron reactions with O_2 may occur. Only the Q_o site semiquinone still features a sufficiently low redox potential to be able to inject an electron into O_2. The question arises why evolution didn't end up with even higher quinone E_m values minimizing also the threat of $O_2^{\bullet -}$ production from this semiquinone species. When considering the integration of the complex in a bioenergetic reaction chain we may come up with two reasons for the universal choice of about +100 mV for high potential quinones, whether they evolved in Bacteria as PQ or UQ or in Archaea as CQ.

First, the E_m upshifts may be limited by the oxidising power of the terminal acceptors. Forward electron transfer from the quinol/semiquinone couple to the light-oxidised pigment of the photosynthetic reaction centre (E_m ca. +500 mV [69]) in the high potential system of *R. sphaeroides* would indeed become thermodynamically unfavorable if the entire redox layout of its bc_1 complex would be further shifted to sufficiently positive values for the semiquinone/quinone couple to

leave the region of facile O_2-reduction. While limited oxidising power of the electron sink at the end of the chain may appear less of a problem in O_2-respiration, it must be kept in mind that the Rieske/cyt*b* complexes also function in anaerobic respiration such as for example the denitrifying pathway in *Paracoccus denitrificans*. The nitrate/nitrite couple's E_m being in the region of +400 mV, the redox constraints exerted by this kind of terminal electron acceptor are likely even more restrictive than those of the photosynthetic systems. The actual E_m-values of high potential quinones indeed seem to represent the best possible compromise between the tendency to move positive in order to minimize superoxide production and the need to keep sufficient thermodynamic driving force towards a variety of terminal electron acceptors.

Secondly, when considering the electron transfer chain from NADH to O_2 the driving force for electron transfer upstream of the Rieske/cyt*b* complex, from NADH to UQ, equals the driving force for the downstream electron transfer from the Rieske cluster to O_2, and amounts to ca 450 mV in both cases. This energy is necessary and sufficient for forward electron transfer coupled to the translocation of two protons over the membrane against the pmf, as realized by complex I and the SoxM/typeA O_2-reductases. A quinone redox potential at +100 mV therefore optimizes the output of proton motive force from the NADH/O_2 couple by allowing the transfer of 5 charges over the membrane for each electron travelling through the three enzymes.

5. Conclusions

Comparing the redox properties of MK- and UQ/PQ-organisms allows a glimpse back in history to the Great Oxidation Event 2.5 billion years ago, when the rise of atmospheric oxygen resulted in an up-shift of the ambient redox potential. Organisms faced the challenge to (a) make use of this powerful electron acceptor and (b) to avoid deleterious reactions with oxygen and reactive oxygen species. They likely responded by an up-shift of the redox potential of the pool quinone by 150 mV and a commensurable increase of the entire set of redox potentials of the cofactors in the Rieske/cyt*b* complex. This global response proved to be not only a highly efficient but thermodynamically the only possible response for the Q-cycle enzyme to this environmental challenge. It allowed a redistribution of the driving forces between electron transfer from NADH to quinone and from the Rieske cluster to O_2 in a way optimizing pmf output, it limited the number of cofactors in the Rieske/cyt*b* complex able to achieve 1-electron reduction of O_2 to only a single one, the Q_o-site semiquinone, while respecting the stringent thermodynamic constraints of Q-cycle function. The role of thermodynamic constraints as evolutionary selection pressure so far received only scant attention in the evolutionary community. They now appear as the dominant factor that shaped the evolutionary transition of the bioenergetic reaction chains during the GOE, leaving only a minor margin for further fine-tunings of selected electrochemical parameters attributable to ROS avoidance.

Transparency Document

The Transparency Document associated with this article can be found, in online version.

Acknowledgments

We thank M. Bauzan (Unité de fermentation, IMM) for cell cultures and F. Rappaport for stimulating discussion. This work was supported by the ANR BisP (ANR-10-BLAN-1506), a PhD fellowship from Université Pierre et Marie Curie (to L.B.), and the Labex Dynamo (ANR-11-LABX-0011-01). EPR facilities at Aix-Marseille University EPR Center receive financial support from the TGE RPE FR3443.

References

[1] B. Schoepp-Cothenet, R. van Lis, A. Atteia, F. Baymann, L. Capowiez, A.L. Ducluzeau, S. Duval, F. ten Brink, M.J. Russell, W. Nitschke, On the universal core of bioenergetics, Biochim. Biophys. Acta 1827 (2013) 79–93.
[2] N. Lane, J.F. Allen, W. Martin, How did LUCA make a living? Chemiosmosis in the origin of life, BioEssays 32 (2010) 271–280.
[3] P. Mitchell, Chemiosmotic coupling in oxidative and photosynthetic phosphorylationReprinted in 2011 in Biochim. Biophys. Acta 1807 (1966) 1507–1538.
[4] A.R. Crofts, S. Hong, C. Wilson, R. Burton, D. Victoria, C. Harrison, K. Schulten, The mechanism of ubihydroquinone oxidation at the Qo-site of the cytochrome *bc*1 complex, Biochim. Biophys. Acta 1827 (2013) 1362–1377.
[5] S. Dröse, U. Brandt, The mechanism of mitochondrial superoxide production by the cytochrome *bc*1 complex, J. Biol. Chem. 283 (2008) 21649–21654.
[6] H. Han, J. Hemp, L.A. Pace, H. Ouyang, K. Ganesan, J.H. Roh, F. Daldal, S.R. Blanke, R.B. Gennis, Adaptation of aerobic respiration to low O_2 environments, Proc. Natl. Acad. Sci. U. S. A. 108 (2011) 14109–14114.
[7] A. Osyczka, C.C. Moser, F. Daldal, P.L. Dutton, Reversible redox energy coupling in electron transfer chains, Nature 427 (2004) 607–612.
[8] V. Rauhamäki, M. Wikström, The causes of reduced proton-pumping efficiency in type B and C respiratory heme-copper oxidases, and in some mutated variants of type A, Biochim. Biophys. Acta 1837 (2014) 999–1003.
[9] P.R. Vennam, N. Fisher, M.D. Krzyaniak, D.M. Kramer, M.K. Bowman, A caged, destabilized, free radical intermediate in the Q-cycle, Chembiochem 14 (2013) 1745–1753.
[10] P.M. Wood, The two redox potentials for oxygen reduction to superoxide, Trends Biochem. Sci. 12 (1987) 250–251.
[11] J.H. Golbeck, B. Kok, Redox titration of electron acceptor Q and the plastoquinone pool in photosystem II, Biochim. Biophys. Acta 547 (1979) 347–360.
[12] H. Zhang, A. Osyczka, P.L. Dutton, C.C. Moser, Exposing the complex III Qo semiquinone radical, Biochim. Biophys. Acta 1767 (2007) 883–887.
[13] M. Schütz, M. Brugna, E. Lebrun, F. Baymann, R. Huber, K.-O. Stetter, G. Hauska, R. Toci, D. Lemesle-Meunier, P. Tron, C. Schmidt, W. Nitschke, Early evolution of cytochrome *bc* complexes, J. Mol. Biol. 300 (2000) 663–675.
[14] A. Hiraishi, Y.K. Shin, J. Sugiyama, *Brachymonas denitrificans* gen. sp. nov., an aerobic chemoorganotrophic bacterium which contains rhodoquinones, and evolutionary relationships of rhodoquinone producers to bacterial species with various quinone classes, J. Gen. Appl. Microbiol. 41 (1995) 99–117.
[15] W. Nitschke, D.M. Kramer, A. Riedel, U. Liebl, From naphtho- to benzoquinones —(r)evolutionary reorganisations of electron transfer chains, in: P. Mathis (Ed.), Photosynthesis: From Light to Biosphere, Vol. I, Kluwer Acad. Publishers, Dordrecht 1995, pp. 945–950.
[16] B. Schoepp-Cothenet, C. Lieutaud, F. Baymann, A. Vermeglio, T. Friedrich, D.M. Kramer, W. Nitschke, Menaquinone as pool quinone in a purple bacterium, Proc. Natl. Acad. Sci. U. S. A. 106 (2009) 8549–8554.
[17] X.-Y. Zhi, J.-C. Yao, S.-K. Tang, Y. Huang, H.-W. Li, W.-J. Li, The futalosine pathway played an important role in menaquinone biosynthesis during early prokaryote evolution, Genome Biol. Evol. 6 (2014) 149–160.
[18] C.A. Partin, S.V. Lalonde, N.J. Planavsky, A. Bekker, O.J. Rouxel, T.W. Lyons, K.O. Konhauser, Uranium in iron formations and the rise of atmospheric oxygen, Chem. Geol. 362 (2013) 82–90.
[19] D. Xia, L. Esser, W.-K. Tang, F. Zhou, Y. Zhou, L. Yu, C.-A. Yu, Structural analysis of cytochrome *bc*1 complexes: implications to the mechanism of function, Biochim. Biophys. Acta 1827 (2013) 1278–1294.
[20] A. Osyczka, C.C. Moser, P.L. Dutton, Fixing the Q-cycle, Trends Biochem. Sci. 30 (2005) 76–182.
[21] J.L. Cape, M.K. Bowman, D.M. Kramer, Understanding the cytochrome *bc* complexes by what they don't do. The Q-cycle at 30, Trends Plant Sci. 11 (2006) 46–55.
[22] A.W. Rutherford, A. Osyczka, F. Rappaport, Back-reactions, short-circuits, leaks and other energy wasteful reactions in biological electron transfer: redox tuning to survive life in O_2, FEBS Lett. 586 (2012) 603–616.
[23] D. Kuila, J.A. Fee, Evidence for a redox-linked ionizable group associated with the [2Fe–2S] cluster of Thermus Rieske protein, J. Biol. Chem. 261 (1986) 2768–2771.
[24] E. Kutoh, N. Sone, Quinol-cytochrome *c* oxidoreductase from the thermophilic bacterium PS3. Purification and properties of a cytochrome *bc*1(b6f) complex, J. Biol. Chem. 263 (1988) 9020–9026.
[25] U. Liebl, A.W. Rutherford, W. Nitschke, Evidence for a unique Rieske iron–sulphur center in *Heliobacterium chlorum*, FEBS Lett. 261 (1990) 427–430.
[26] U. Liebl, S. Pezennec, A. Riedel, E. Kellner, W. Nitschke, The Rieske FeS center from the gram-positive bacterium PS3 and its interaction with the menaquinone pool studied by EPR, J. Biol. Chem. 267 (1992) 14068–14072.
[27] D.M. Kramer, B. Schoepp, U. Liebl, W. Nitschke, Cyclic electron transfer in *Heliobacillus mobilis* involving a menaquinol-oxidizing cytochrome *bc* complex and an RCI-type reaction center, Biochemistry 36 (1997) 4203–4211.
[28] M. Brugna, D. Albouy, W. Nitschke, Diversity of cytochrome *bc* complexes: example of the Rieske protein in green sulfur bacteria, J. Bacteriol. 180 (1998) 3719–3723.
[29] N. Sone, M. Sekimachi, E. Kutoh, Identification and properties of a quinol oxidase super-complex composed of a *bc*1 complex and cytochrome oxidase in the thermophilic bacterium PS3, J. Biol. Chem. 262 (1987) 15386–15391.
[30] N. Sone, Y. Yanagita, A cytochrome *aa*3-type terminal oxidase of a thermophilic bacterium: purification, properties and proton pumping, Biochim. Biophys. Acta 682 (1982) 216–226.
[31] C. von Wachenfeldt, L. Hederstedt, *Bacillus subtilis* 13-kilodalton cytochrome *c*-550 encoded by cccA consists of a membrane-anchor and a heme domain, J. Biol. Chem. 265 (1990) 13939–13948.

[32] B. van Gelder, E.C. Slater, The extinction coefficient of cytochrome *c*, Biochim. Biophys. Acta 58 (1962) 593–595.
[33] P.L. Dutton, Oxidation–reduction potential dependence of the interaction of cytochromes, bacteriochlorophyll and carotenoids at 77 K in chromatophores of *Chromatium* D and *Rhodopseudomonas gelatinosa*, Biochim. Biophys. Acta 226 (1971) 63–80.
[34] F. Baymann, D.A. Moss, W. Mäntele, An electrochemical assay for the characterization of redox proteins from biological electron-transfer chains, Anal. Biochem. 199 (1991) 269–274.
[35] N. Sone, Y. Fujiwara, Heme-o can replace heme-a in the active-site of cytochrome-*c*-oxidase from thermophilic bacterium PS3, FEBS Lett. 288 (1991) 154–158.
[36] S. Duval, J.M. Santini, W. Nitschke, R. Hille, B. Schoepp-Cothenet, The small subunit AroB of arsenite oxidase: lessons on the [2Fe2S] Rieske protein superfamily, J. Biol. Chem. 285 (2010) 20442–20451.
[37] E. Hurt, G. Hauska, Identification of the polypeptides in the cytochrome *b6/f* complex from spinach chloroplasts with redox-center-carrying subunits, J. Bioenerg. Biomembr. 14 (1982) 405–425.
[38] J. Yu, L. Hederstedt, P.J. Piggot, The cytochrome *bc* complex (menaquinone:cytochrome *c* reductase) in *Bacillus subtilis* has a nontraditional subunit organization, J. Bacteriol. 1777 (1995) 6751–6760.
[39] A.L. Ducluzeau, E. Chenu, L. Capowiez, F. Baymann, The Rieske/cytochrome *b* complex of Heliobacteria, Biochim. Biophys. Acta 1777 (2008) 1140–1146.
[40] J. Alric, Y. Pierre, D. Picot, J. Lavergne, F. Rappaport, Spectral and redox characterization of the heme ci of the cytochrome *b6f* complex, Proc. Natl. Acad. Sci. U. S. A. 102 (2005) 15860–15865.
[41] F. Baymann, F. Giusti, D. Picot, W. Nitschke, The ci/bH moiety in the *b6f* complex studied by EPR: a pair of strongly interacting hemes, Proc. Natl. Acad. Sci. U. S. A. 104 (2007) 519–524.
[42] H. Zhang, A. Primak, J. Cape, M.K. Bowman, D.M. Kramer, W.A. Cramer, Characterization of the high spin heme x in the cytochrome *b6f* complex of oxygenic photosynthesis, Biochemistry 43 (2004) 16329–16336.
[43] D. Stroebel, Y. Choquet, J.-L. Popot, D. Picot, An atypical haem in the cytochrome *b6f* complex, Nature 426 (2003) 413–418.
[44] Y. Fujiwara, M. Oka, T. Hamamoto, N. Sone, Cytochrome *c*-551 of the thermophilic bacterium PS3, DNA sequence and analysis of the mature cytochrome, Biochim. Biophys. Acta 1144 (1993) 213–219.
[45] P. Nicholls, L.C. Petersen, Haem–haem interactions in cytochrome *aa*3 during the anaerobic–aerobic transition, Biochim. Biophys. Acta 357 (1974) 462–467.
[46] H. Yue, Y. Kang, H. Zhang, X. Gao, R.E. Blankenship, Expression and characterization of the diheme cytochrome *c* subunit of the cytochrome *bc* complex in *Heliobacterium modesticaldum*, Arch. Biochem. Biophys. 517 (2012) 131–137.
[47] Y. Neehaul, Study of Proteins in the Respiratory Chain by IR Spectroscopy and Electrochemistry(phD thesis) Institut de Physique et Chimie des Matériaux, Strasbourg, France, 2012.
[48] P. Infossi, E. Lojou, J.-P. Chauvin, G. Herbette, M. Brugna, M.-T. Giudici-Orticoni, *Aquifex aeolicus* membrane hydrogenase for hydrogen biooxidation: role of lipids and physiological partners in enzyme stability and activity, Int. J. Hydrog. Energy 35 (2010) 10778–10789.
[49] M. Schütz, B. Schoepp-Cothenet, E. Lojou, M. Woodstra, D. Lexa, P. Tron, A. Dolla, M.-C. Durand, K.O. Stetter, F. Baymann, The naphthoquinol oxidizing cytochrome *bc*1 complex of the hyperthermophilic Knallgasbacterium *Aquifex aeolicus*: properties and phylogenetic relationships, Biochemistry 42 (2003) 10800–10808.
[50] P. Mitchell, Possible molecular mechanisms of proton motive function of cytochrome systems, J. Theor. Biol. 62 (1976) 327–367.
[51] J.A. Cooley, A.G. Roberts, M.K. Bowman, D.M. Kramer, F. Daldal, The raised midpoint potential of the [2Fe2S] cluster of cytochrome *bc*1 is mediated by both the Qo site occupants and the head domain position of the Fe–S protein subunit, Biochemistry 43 (2004) 2217–2227.
[52] D.E. Robertson, R.C. Prince, J.R. Bowyer, K. Matsuura, P.L. Dutton, T. Ohnishi, Thermodynamic properties of the semiquinone and its binding site in the ubiquinol-cytochrome *c* (c2) oxidoreductase of respiratory and photosynthetic systems, J. Biol. Chem. 259 (1984) 1758–1763.
[53] G. Kurisu, H. Zhang, J.L. Smith, W.A. Cramer, Structure of the cytochrome *b6f* complex of oxygenic photosynthesis: tuning the cavity, Science 302 (2003) 1009–1014.
[54] D. Nicholls, S. Fergusson, Bioenergetics, fourth ed. Academics, Amsterdam, 2013.
[55] A. Malnoë, F.A. Wollman, C. de Vitry, F. Rappaport, Photosynthetic growth despite a broken Q-cycle, Nat. Commun. 2 (2011) 301.
[56] M. Sarewicz, A. Borek, E. Cieluch, M. Swierczek, A. Osyczka, Discrimination between two possible reaction sequences that create potential risk of generation of deleterious radicals by cytochrome *bc*1; implications for the mechanism of superoxide production, Biochim. Biophys. Acta 1797 (2010) 1820–1827.
[57] A. Borek, M. Sarewicz, A. Osyczka, Movement of the iron–sulfur head domain of cytochrome *bc*1 transiently opens the catalytic Qo site for reaction with oxygen, Biochemistry 47 (2008) 12365–12370.
[58] L. Carraretto, E. Formentin, E. Teardo, V. Checchetto, M. Tomiziolo, T. Morosinotto, G.M. Giacometti, G. Finazzi, I. Szabo, A thylacoid-located two-pore K^+ channel controls photosynthetic light utilization in plants, Science 342 (2013) 114–118.
[59] W.J. Ingledew, J.G. Cobley, A potentiometric and kinetic study on the respiratory chain of ferrous-iron grown *Thiobacillus ferrooxidans*, Biochim. Biophys. Acta 590 (1980) 141–158.
[60] W.J. Ingledew, *Thiobacillus ferrooxidans*. The bioenergetics of an acidophilic chemolitotroph, Biochim. Biophys. Acta 683 (1982) 89–117.
[61] A. Elbehti, W. Nitschke, P. Tron, C. Michel, D. Lemesle-Meunier, Redox components of cytochrome *bc*-type enzymes in acidophilic prokaryotes. I. Characterization of the cytochrome *bc*1-type complex of the acidophilic ferrous ion-oxidizing bacterium *Thiobacillus ferrooxidans*, J. Biol. Chem. 274 (1999) 16760–16765.
[62] S. Pintscher, P. Kuleta, E. Cieluch, B. Arkadiusz, M. Sarewicz, A. Osyczka, Tuning of hemes *b* equilibrium redox potential is not required for cross-membrane electron transfer, J. Biol. Chem. (2016), http://dx.doi.org/10.1074/jbc.M1115.712307.
[63] J.L. Cape, M.K. Bowman, D.M. Kramer, A semiquinone intermediate generated at the Qo site of the cytochrome *bc*1 complex: importance for the Q-cycle and superoxide production, Proc. Natl. Acad. Sci. U. S. A. 104 (2007) 7887–7892.
[64] L. Bleier, S. Dröse, Superoxide generation by complex III: from mechanistic rationales to functional consequences, Biochim. Biophys. Acta 1827 (2013) 1320–1331.
[65] P. Lanciano, B. Khalfaoui-Hassani, N. Selamoglu, A. Ghelli, M. Rugolo, F. Daldal, Molecular mechanisms of superoxide production by complex III: a bacterial versus human mitochondrial comparative case study, Biochim. Biophys. Acta 1827 (2013) 1322–1329.
[66] D. Baniulis, S.S. Hasan, J.T. Stofleth, W.A. Cramer, Mechanism of enhanced superoxide production in the cytochrome *b6f* complex of oxygenic photosynthesis, Biochemistry 52 (2013) 8975–8983.
[67] P.M. Wood, The potential diagram for oxygen at pH 7, Biochem. J. 253 (1988) 287–289.
[68] G. Hauska, E. Hurt, N. Gabellini, W. Lockau, Comparative aspects of quinol-cytochrome *c*/plastocyanin oxidoreductases, Biochim. Biophys. Acta 726 (1983) 97–133.
[69] J.C. Williams, R.G. Alden, H.A. Murchison, J.M. Peloquin, N.W. Woodbury, J.P. Allan, Effects of mutations near the bacteriochlorophylls in reaction centers from *Rhodobacter sphaeroides*, Biochemistry 31 (1992) 11029–11037.
[70] K. Takamiya, P.L. Dutton, Ubiquinone in *Rhodopseudomonas sphaeroides*; some thermodynamic properties, Biochim. Biophys. Acta 546 (1979) 1–16.
[71] G.C. Wagner, R.J. Kassner, D. Kamen, Redox potentials of certain vitamins K: implications for a role in sulfite reduction by obligately anaerobic bacteria, Proc. Natl. Acad. Sci. U. S. A. 71 (1974) 253–256.
[72] S.W. Meinhardt, A.R. Crofts, The role of cytochrome *b*-566 in the electron transfer chain of *Rhodopseudomonas sphaeroides*, Biochim. Biophys. Acta 723 (1983) 219–230.
[73] R.C. Prince, J.G. Lindsay, P.L. Dutton, The Rieske iron–sulfur center in mitochondrial and photosynthetic systems: Em/pH relationships, FEBS Lett. 51 (1975) 108–111.
[74] E. Denke, T. Merbitz-Zahradnik, O.M. Hatzfeld, C.H. Snyder, T.A. Link, B.L. Trumpower, Alteration of the midpoint potential and catalytic activity of the Rieske iron–sulfur protein by changes of amino acids forming hydrogen bonds to the iron–sulfur cluster, J. Biol. Chem. 273 (1998) 9085–9093.
[75] F.A. Rotsaert, R. Covian, B.L. Trumpower, Mutations in cytochrome *b* that affect kinetics of the electron transfer reactions at center N in the yeast cytochrome *bc*1 complex, Biochim. Biophys. Acta 1777 (2008) 239–249.
[76] D.E. Robertson, H. Ding, P.R. Chelminski, C. Slaughter, J. Hsu, C. Moomaw, M. Tokito, F. Daldal, P.L. Dutton, Hydroubiquinone-cytochrome *c*2 oxidoreductase from *Rhodobacter capsulatus*: definition of a minimal, functional isolated preparation, Biochemistry 32 (1993) 1310–1317.
[77] Y. Kabashima, N. Sone, T. Kusumoto, J. Sakamoto, Purification and characterization of malate:quinone oxidoreductase from thermophilic *Bacillus* sp. PS3, J. Bioenerg. Biomembr. 45 (2013) 131–136.
[78] P.E. Thomas, D. Ryan, W. Levin, An improved staining procedure for the detection of the peroxidase activity of cytochrome *p*-450 on sodium dodecyl sulfate polyacrylamide gels, Anal. Biochem. 75 (1976) 168–176.